Pavel KARBAN, František MACH, Ivo DOLEŽEL

University of West Bohemia in Plzeň, Czech Republic

Hard-Coupled Model of Induction Heating of Cylindrical Nonmagnetic Billets Rotating in System of Permanent Magnets

Abstract. *A new technology of induction heating of nonmagnetic cylindrical billets by their rotation in static magnetic field produced by a system of permanent magnets is presented and modeled. Analyzed is effectiveness of the process (particularly the time necessary for reaching a prescribed average temperature) in the dependence of the arrangement of the permanent magnets. The methodology is illustrated by a typical example.*

Streszczenie. *Zaprezentowano owa technologia grzania indukcyjnego sztabek cylindrycznych niemagnetycznych poprzez ich rotację t statycznym polu magnetycznym wytwarzanym przez system magnesów trwałych jest . Analizowana jest skuteczność systemu, ale też czas konieczny do osiągnięcia założonej średniej temperatury w zależności od ustawienia magnesów trwałych. Przedstawiona technologia została zilustrowana typowym przykładem. (**Silnie sprzężony model grzania indukcyjnego cylindrycznych niemagnetycznych sztabek wirujących systemie magnesów trwałych**)*

Keywords: induction heating, cylindrical billets, permanent magnets, hard-coupled formulation.
Słowa kluczowe: grzanie indukcyjne, cylindryczna sztabka, magnesy trwałe, magnesy trwałe, sformułowanie silnie srzężone

Introduction

Induction heating of cylindrical billets of nonmagnetic metals (mostly aluminum) is a technological process used, for example, for their softening before hot forming [1–2]. The process of heating can be realized in several principal manners.

The classical way consists in heating of unmoving billet inside a massive cylindrical harmonic current-carrying inductor. But the effectiveness of this way is rather low due to the Joule losses in the inverter and inductor (that must be transferred away by an appropriate cooling medium). The efficiency of the process does not exceed 50–60 %.

Several years ago an alternative way of heating was suggested, based on rotation of the billet in static magnetic field generated by suitably arranged direct current-carrying inductors [3–4]. The efficiency of this way is higher and ranges between 70–80 %. But the construction of the system is rather complicated because of very high field currents, which usually requires supplementary superconducting cryogenic systems. Nevertheless, this technology was successfully introduced in several industrial companies [5] and seems to be sufficiently good even for billets of higher diameters (up to about 20 cm).

The authors of this paper started with research of another version of this manner suitable mainly for billets of lower diameters, now up to about 10 cm. Here the static magnetic field is generated by appropriately arranged high-parameter permanent magnets. The version is characterized by no Joule losses and the only losses in the system are caused by the drag torque due to interaction between the static magnetic field and currents induced in the rotating billet. In this case, efficiency could reach even 85 %. The first study of the system describing induction heating of a thin-wall aluminum pipe was published in [6], several results were validated experimentally.

The paper deals with a thorough analysis of the induction heating of massive aluminum billets realized in this manner. Determined are the main operation characteristics of the process such as the velocity of heating, drag torque and other quantities of higher importance.

Definition of the problem

The investigated arrangement (representing a prototype that is to be built in the cooperating industrial plant) is depicted in Fig. 1. It is sufficiently long in the axial direction, so that the distribution of magnetic and temperature fields in it may be considered 2D. The aluminum billet **1** rotates (at angular velocity ω) in the static part of the system consisting of permanent magnets **2** fixed on ferromagnetic shoulders **3.** The permanent magnets are embedded in a good thermal insulation **4** that prevents them from excessive heating due to convection from the billet.

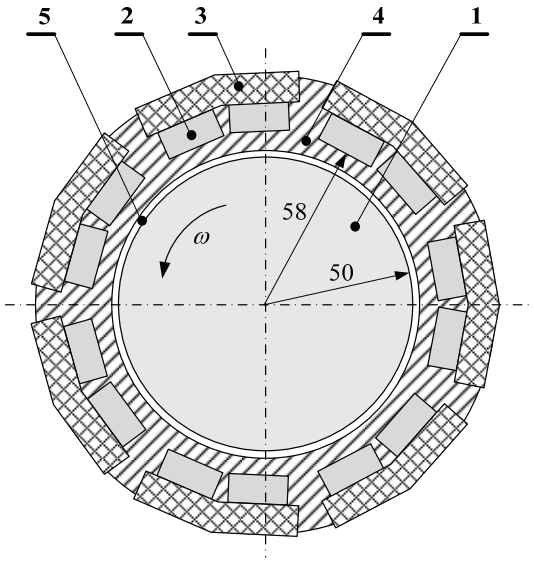

Fig. 1. The investigated arrangement (all dimensions in mm): **1**–rotating heated billet, **2**–permanent magnets, **3**–ferromagnetic shoulders, **4**–thermal insulation, **5**–air gap

The disposition of the permanent magnets on ferromagnetic shoulders is depicted in Fig. 2.

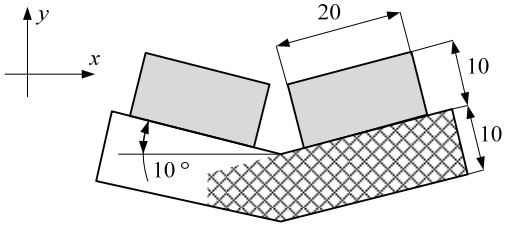

Fig. 2. Disposition of permanent magnets on ferromagnetic shoulders (dimensions in mm)

The goal is to map the distribution of magnetic field in the system, distribution of induced currents in the rotating billet, drag torque acting on the billet, and time evolution of

its local and average temperatures. The orientation of the permanent magnets in the system may change.

The problem is solved in the hard-coupled formulation (i.e., both physical fields are solved simultaneously, with one stiffness matrix). All important nonlinearities are taken into account.

Continuous mathematical model

Magnetic field in the system may advantageously be described by the magnetic vector potential. Its distribution is given by the solution of the equation [7]

$$\operatorname{curl}\left(\frac{1}{\mu}\operatorname{curl}\boldsymbol{A}-\boldsymbol{H}_{\mathrm{c}}\right)-\gamma\boldsymbol{v}\times\operatorname{curl}\boldsymbol{A}=\boldsymbol{0}, \tag{1}$$

where γ is the electrical conductivity, $\boldsymbol{v}$ stands for the vector of the local velocity of rotation, and $\boldsymbol{H}_{\mathrm{c}}$ is the coercive force (this is only considered in the domain of the permanent magnets, elsewhere it vanishes). A sufficiently distant artificial boundary is described by the Dirichlet condition $\boldsymbol{A}=\boldsymbol{0}$.

The currents induced in the billet are characterized by the density

$$\boldsymbol{J}_{\mathrm{ind}}=\gamma\boldsymbol{v}\times\operatorname{curl}\boldsymbol{A} \tag{2}$$

that produces the volumetric Joule losses

$$w_{\mathrm{J}}=\left|\boldsymbol{J}_{\mathrm{ind}}\right|^{2}/\gamma \tag{3}$$

representing the sources of heat.

The time-dependent distribution of the temperature obeys the heat transfer equation in the form [8]

$$\operatorname{div}\left(\lambda\operatorname{grad}T\right)=\rho c\cdot\left(\frac{\partial T}{\partial t}+\boldsymbol{v}\cdot\operatorname{grad}T\right)-w_{\mathrm{J}}, \tag{4}$$

where λ is the thermal conductivity, ρ denotes the specific mass, and c stands for the specific heat. The boundary condition respects both the convection and radiation. All physical parameters of the system are generally functions of the temperature.

Numerical solution

The numerical solution of the problem is realized by a fully adaptive higher-order finite element method [9], whose algorithms are implemented into our own codes Hermes [10] and Agros [11]. Both codes have been developed in our group for a couple of years.

The codes written in C++ are intended for monolithic numerical solution of systems of generally nonlinear and nonstationary second-order partial differential equations (rewritten into corresponding weak formulations) whose principal purpose is modeling of complex physical problems. While Hermes is a library containing the most advanced procedures and algorithms for the numerical processing of the task, Agros represents a powerful preprocessor and postprocessor. Both codes are freely distributable under the GNU General Public License. The most important (and often quite unique) features of the codes follow:

- Solution of the system of PDEs is carried out monolithically, which means that the resultant numerical scheme is characterized by just one stiffness matrix.
- Fully automatic *hp*-adaptivity. In every iteration step the solution is compared with the reference solution (realized on an approximately twice finer mesh), and the distribution of error is then used for selection of candidates for adaptivity. Based on sophisticated and subtle algorithms the adaptivity is realized either by a subdivision of the candidate element or by its description by a polynomial of a higher order.
- Each physical field can be solved on a different mesh that best corresponds to its particulars. This is of great importance, for instance, for respecting skin effect in the electromagnetic field, boundary layers in the field of flow problems, etc. Special higher-order techniques of mapping are then used to avoid any numerical errors in the process of assembly of the stiffness matrix.
- In nonstationary processes every mesh can change in time, in accordance with the real evolution of the corresponding physical quantities.
- No problems with the hanging nodes [12] appearing on the boundaries of subdomains whose elements have to be refined. Usually the hanging nodes bring about a considerable increase of the number of the degrees of freedom (DOFs). The code contains higher-order algorithms for respecting these nodes without any need of an additional refinement of the external parts neighboring with the refined subdomain.
- Curved elements able to replace curvilinear parts of any boundary by a system of circular or elliptic arcs. These elements mostly allow reaching highly accurate results near the curvilinear boundaries with very low numbers of DOFs.

The weak forms of equations (1) and (4) for the coordinate system x, y (in which all the computations were realized) are

$$\begin{aligned}&\int_{\Omega}\frac{1}{\mu}\left(\frac{\partial A_z}{\partial x}\cdot\frac{\partial w}{\partial x}+\frac{\partial A_z}{\partial y}\cdot\frac{\partial w}{\partial y}\right)\mathrm{d}S+\\&+\int_{\Omega}\gamma\left(A_z v_x\frac{\partial w}{\partial x}+A_z v_y\frac{\partial w}{\partial y}\right)\mathrm{d}S=\\&=-\int_{\Omega}\frac{1}{\mu}\left(B_{\mathrm{r},y}\cdot\frac{\partial w}{\partial x}-B_{\mathrm{r},x}\cdot\frac{\partial w}{\partial y}\right)\mathrm{d}S-\int_{\Gamma}\left(Kw\right)\mathrm{d}l,\end{aligned} \tag{5}$$

$$\begin{aligned}&\int_{\Omega}\lambda\left(\frac{\partial T}{\partial x}\cdot\frac{\partial w}{\partial x}+\frac{\partial T}{\partial y}\cdot\frac{\partial w}{\partial y}\right)\mathrm{d}S+\int_{\Omega}\rho c_{\mathrm{p}}\frac{\partial T}{\partial t}w\,\mathrm{d}S-\\&-\int_{\Omega}\rho c_{\mathrm{p}}T\left(v_x\frac{\partial w}{\partial x}+v_y\frac{\partial w}{\partial y}\right)\mathrm{d}S+\\&+\int_{\Gamma}\alpha T w\,\mathrm{d}l=\int_{\Omega}p_{\mathrm{J}}w\,\mathrm{d}S+\int_{\Gamma}\left(\alpha T_0+g\right)w\,\mathrm{d}l.\end{aligned} \tag{6}$$

Here Ω denotes the cross section of the investigated area and Γ is its boundary. Symbol A_z is the z-component of magnetic vector potential, v_x and v_y are the components of velocity $\boldsymbol{v}$ in the corresponding directions, and finally $B_{\mathrm{r},x}$ and $B_{\mathrm{r},y}$ stand for the components of remanence $\boldsymbol{B}_{\mathrm{r}}$. Symbol α denotes the generalized coefficient of convective heat transfer, T_0 is temperature of external air, and K and g are appropriate constants. Finally, w is a suitable testing function of polynomial character satisfying the boundary conditions of the problem.

Illustrative example

The ferromagnetic shoulders are made of carbon steel 12 040. Its magnetization characteristic together with the temperature--dependent dependencies of material parameters of aluminum can be found in [6].

The permanent magnets NdBFe are of type VMM10 (probably the strongest permanent magnets available in the market). Their average relative permeability in the second quadrant $\mu_{ra} = 1.21$ and their remanence $B_r = 1.41$ T.

The thermal insulation is formed by glass wool of very poor thermal conductivity. The process of heating the billet is then practically adiabatic (when the front effects would be neglected).

In accordance with Fig. 1, the number of shoulders is 7 and the number of permanent magnets is 14. We investigated two basic possibilities differing by their orientation.

The orientation of permanent magnets in the first case is schematically depicted in Fig. 3, left part (neighboring magnets on two neighboring shoulders have the same orientation). As the number of shoulders is odd, the arrangement cannot be, in principle, quite symmetric. In the second case, the orientations of permanent magnets on all shoulders are the same, which is obvious from Fig. 3, right part.

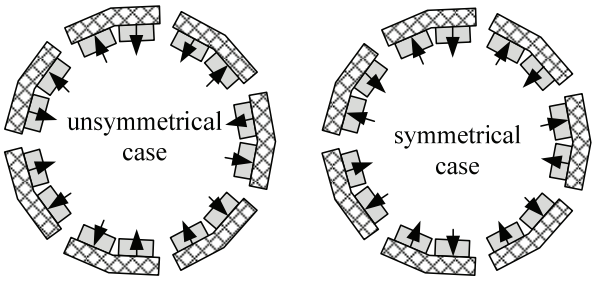

Fig. 3. Two investigated options differing by the orientation of permanent magnets

The mesh for computation of magnetic field was generated using the adaptive process that took 12 steps. The corresponding convergence curve (dependence of the relative error η on the number of DOFs) is shown in Fig. 4 (the prescribed tolerance was 1 % as is marked by the horizontal line).

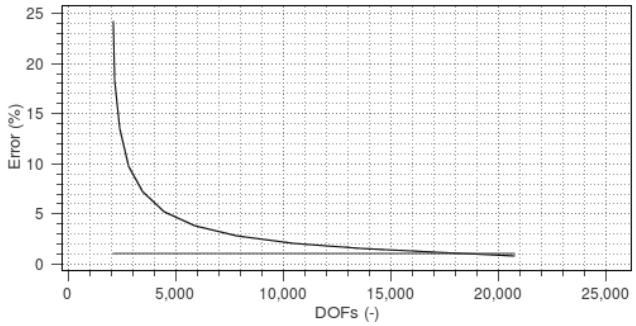

Fig. 4. Convergence curve of the process of adaptivity

Another curve giving the idea about the growth of DOFs in the course of the adaptivity process is given in Fig. 5.

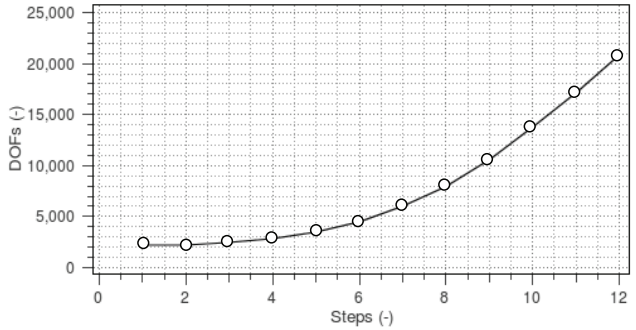

Fig. 5. Growth of DOFs in particular steps of the adaptivity process

The final mesh is depicted in Fig. 6 (we used exclusively the triangular elements, whose sides were curved when they laid on any circular interface. The numbers in rectangles on the right denote the degree of polynomials in particular triangular elements. The number of revolution of the billet $n = 750$ /min.

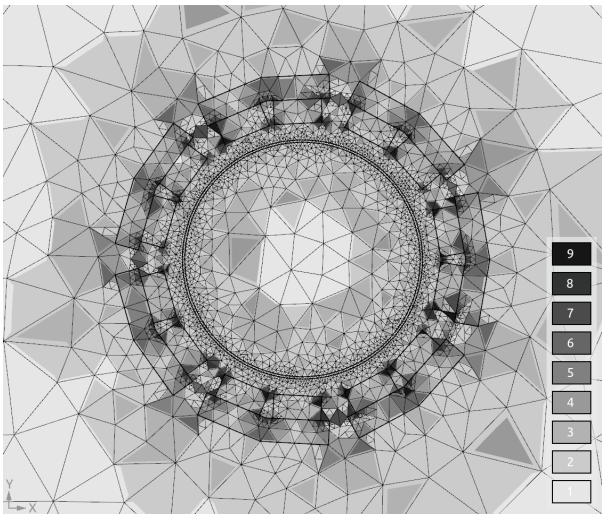

Fig. 6. Mesh after the process of adaptivity used for the computation of magnetic field in the system

The computations of both arrangements in Fig. 3 provide quite different results. The corresponding field maps are depicted in Fig. 7. Its upper part shows the magnetic field for the arrangement corresponding to the unsymmetrical case and the lower part depicts an analogous distribution corresponding to the symmetrical case.

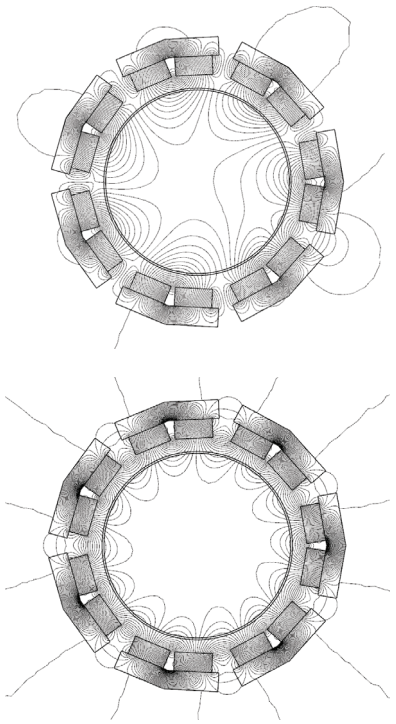

Fig. 7. Maps of magnetic field: unsymmetrical case – up, symmetrical case – down

From the viewpoint of the velocity of heating, more advantageous is the unsymmetrical case that provides higher values of the volumetric Joule losses. The dependence of the average temperature of the billet on time is for both cases depicted in Fig. 8.

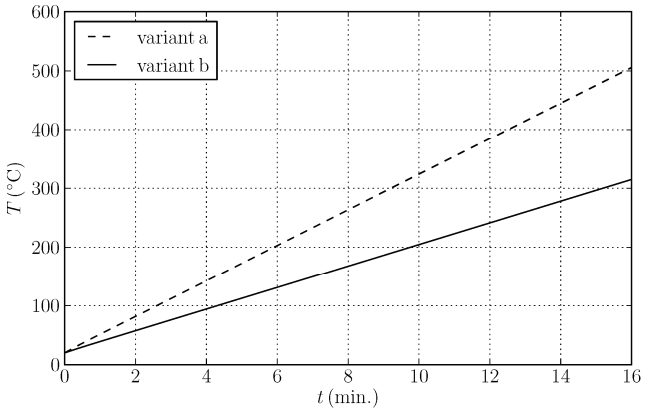

Fig. 8. Average temperature of the billet versus time (variant a - unsymmetrical case, variant b - symmetrical case)

Other items that are necessary to be dealt with, are the drag torque T_d acting on the billet, and efficiency ε of the process.

This drag torque is produced by the interaction between the primary magnetic field generated by the permanent magnet and eddy currents induced in the billet. In case of the unsymmetrical arrangement, its value is 159.5 Nm per one meter of length of the billet, while in case of the symmetrical arrangement we obtain only 95.5 Nm per one meter of length. It means that for faster heating (unsymmetrical case) we have to use a much stronger motor.

The mechanical energy W_m delivered to the system that causes heating of the billet of length $1\,\mathrm{m}$ to, for example, temperature $T = 300$ °C, may approximately (other losses of all kinds are neglected) be calculated in the following way:

$$W_\mathrm{m} = Pt = T_\mathrm{d}\omega t_\mathrm{T},$$

where P is the mechanical output of the machine and t_T is the time of heating to the mentioned temperature. For the unsymmetrical case this time $t_\mathrm{T} = 548\,\mathrm{s}$, for the symmetrical case $t_\mathrm{T} = 912\,\mathrm{s}$. The corresponding energies W_m are now $6.840\,\mathrm{MJ}$ and 6.841 MJ, respectively. Thus, the values are very similar. The thermal energy necessary Q for heating of the billet of length $1\,\mathrm{m}$ from the initial temperature $T_0 = 20\,°\mathrm{C}$ to average temperature $T = 300$ °C follows from the formula

$$Q = mc\left(T - T_0\right) = \rho c V\left(T - T_0\right),$$

which for the aluminum billet of the given dimensions provides about 5.601 MJ.

A rough value of efficiency (other losses are not considered) is

$$\varepsilon = Q / W_\mathrm{m},$$

which gives about 81.9 %. All the above values are listed in Tab. 1.

Conclusion

The higher-order finite element method is a powerful and precise tool for numerical solution of complex physical phenomena. The model of induction heating provided realistic results showing that even relatively massive billets may successfully be heated by their rotation in magnetic field produced by a system of permanent magnets.

Next work in the field must be aimed at the optimization techniques whose aim would be the design of the most advantageous arrangements from the viewpoint of the velocity of heating, drag torque and overall efficiency of the system. The principal way consists in considering a thinner gap between the billet and permanent magnets.

Table 1. Integral values of the investigated heating process

quantity	unit	unsymm. case	symm. case
drag torque T_d	Nm/m	159.5	95.5
angular velocity ω	rad/s	78.5398	78.5398
mechanical power P of the motor	kW	12.527	7.501
difference of temperatures ΔT	°C	280	280
time of heating t_T	s	546	912
average heat capac. of aluminum ρc	MJ/m^{3}K	2,55	2.55
mech. energy W_m	MJ	6.840	6.841
delivered heat Q	MJ	5.601	5.601
efficiency ε	-	0.819	0.819

Acknowledgement

This work was supported by the European Regional Development Fund and Ministry of Education, Youth and Sports of the Czech Republic under the project No. CZ.1.05/2.1.00/03.0094 – RICE, by the Grant project IAA100760702 (GAASCR), Grant project P102/10/0216 (GACR) and Research Plan MSM 6840770017.

REFERENCES

[1] Rudnev, V., Loveless, D., Cook, R., Black, M.: *Handbook of Induction Heating*. Marcel Dekker, Inc., New York, 2003.

[2] Davies, E., J.: *Induction Heating Handbook*. McGraw-Hill, New York, 1979.

[3] Lupi S., Forzan, M.: *A Promising High Efficiency Technology for the Induction Heating of Aluminium Billets*. Proc. UIE Krakow, Poland, pp. 19–20, 2008.

[4] Zlobina M., Nacke B., Nikonarov, A.: *Electromagnetic and Thermal Analysis of Induction Heating of Billets by Rotation in DC Magnetic Field*, Proc. UIE Krakow, Poland, pp. 21–22, 2008.

[5] http://www.weseralu.de.

[6] Karban, P., Mach, F., Doležel, I.: *Induction Heating of Non magnetic Cylindrical Billets by Rotation in Magnetic Field Produced by Static Permanent Magnets*. Przeglad Elektrotechniczny (Electrical Review) 86, No. 12, pp. 53–56, 2010.

[7] Kuczmann, M.: Iványi, A.: *The Finite Element Method in Magnetics*. Akademiai Kiado, Budapest, 2008.

[8] Holman, J.P.: *Heat Transfer*. McGrawHill, NY, 2002

[9] Šolín, P., Segeth, K., Doležel, I.: *Higher-Order Finite Element Methods*. Chapman & Hall/CRC, Boca Raton, USA, 2003.

[10] http://hpfem.org.

[11] http:// agros2d.org.

[12] Šolín, P., Červený, J., Doležel, I.: *Arbitrary-Level Hanging Nodes and Automatic Adaptivity in the hp-FEM*. Math. Comput. Simul. 77, No. 1, pp. 117–132, 2008.

***Authors**: Ing. Pavel Karban, Ph.D., University of West Bohemia, Faculty of Electrical Engineering, Univerzitní 26, 306 14 Plzeň, Czech Republic, E-mail: karban@kte.zcu.cz. Ing. František Mach, University of West Bohemia, Faculty of Electrical Engineering, Univerzitní 26, 306 14 Plzeň, Czech Republic, E-mail: mach.frantisek@gmail.com. Prof. Ing. Ivo Doležel, CSc., Academy of Sciences of the Czech Republic, Institute of Thermomechanics, v.v.i., Dolejškova 5, 182 00 Praha 8, Czech Republic, E-mail: dolezel@it.cas.cz.*